Proceedings of the International Conference on Industrial Engineering and Operations Management

Publisher: IEOM Society International, USA DOI: 10.46254/BA08.20250236
Published: December 20, 2025

Hot-Cracking Susceptibility of Fe-C-Mn Steels: Insights from MatCalc Scheil Simulation

Md. Fardous Hasan Bappy
Materials Science and Engineering Department
Rajshahi University of Engineering and Technology, Rajshahi, Bangladesh
fardousbappy23@gmail.com

Abdullah-Al-Mazed Khan
Materials Science and Engineering Department
Rajshahi University of Engineering and Technology, Rajshahi, Bangladesh
abdullah.khan@mse.ruet.ac.bd

Md. Emran Hossain
Mechanical Engineering Department
Chittagong University of Engineering and Technology, Chittagong, Bangladesh
emran.cuet@gmail.com

Arnika Tabassum Arni
Materials Science and Engineering Department
Rajshahi University of Engineering and Technology, Rajshahi, Bangladesh
tabassum.arnika210@gmail.com

Abstract

Hot cracking is a serious defect that may appear in steels during solidification due to thermal and mechanical stresses which break the thin liquid films between the dendrites. This contribution proposes a new, purely thermodynamics-based computational approach to assess the hot cracking susceptibility of Fe-C-Mn alloys using MatCalc, a CALPHAD-driven software. The ME-Fe database was used to simulate non-equilibrium solidification under Scheil-Gulliver conditions for nine alloy compositions ranging in 0.10-0.80 wt.% C and 0.50-1.50 wt.% Mn. Key parameters comprising the thermodynamic output are freezing range, final liquid fraction, solidification path angle, and final liquid composition. From these parameters, a composite Hot-Cracking Index (HCI) was formulated which may be applied to classify these alloys into susceptibility categories. Carbon was found to be the most prevailing factor; increasing C widens the solidification range and strengthens solute segregation. Manganese had a weaker but still noticeable effect, mainly due to its strong control of the persistence of the final liquid film. A high-risk composition was identified close to 0.80C-1.5Mn, while a safer region was found around 0.10C-1.0Mn. The approach is simple, reproducible, and provides an opportunity for material selection based on thermodynamic behavior; it therefore contributes significantly to alloy design and gives useful guidance for future experimental investigations.

Keywords
Hot Cracking, Solidification, Fe-C-Mn Steels, CALPHAD, MatCalc.

1. Introduction

Hot-cracking, which is also known as solidification cracking, is a historical metallurgical defect that takes place at the very end of solidification in steels. These are the times when a dendritic structure coexists with the necessary thin films of liquid between the dendrites that feed and compensate for thermal shrinkage's (Yusof and Jamaluddin 2014) . If such fragile liquid pathways break under thermal contraction or stress, the formation of cracks leads to the drastic reduction of mechanical performance and structural reliability (Liu et al. 2024). The recurring nature of such failures is becoming more pronounced with the development of new manufacturing techniques like high-energy beam welding and laser additive manufacturing, where rapid thermal cycles and steep gradients play an important role in the magnitude of the risk (Klimpel 2024). The prediction of hot-cracking susceptibility has therefore turned into a major concern in the areas of alloy design and processing. Various thermodynamic descriptors have been put forward to describe the states that induce cracking. One of the main factors is obviously the solidification range ($\Delta T = T_{liq} – T_{sol}$), which controls the time of the presence of the mushy zone (Salge et al. 2020, Dovgyy et al. 2021). A wide ΔT reflects a long period of solid and liquid phases together, thus there is an increasing risk that the thermal strains will coincide with the weak liquid films. Other significant parameters are late-stage liquid fractions close to the solidus, which indicate the amount of liquid that can either heal or feed the microcracks Hu et al. (2024), and the final feeding slope, which illustrates the rapidity with which the interdendritic liquid disappears in the last freezing stages. Moreover, the separation of some elements, e.g., carbon and manganese, into the last liquid has been mentioned as one of the main reasons for this since it not only reduces the melting point in that area but also increases constitutional undercooling(Major 2006, Ma et al. 2023). The knowledge acquired through experiments has been tremendous but it has also been very resource-consuming and sometimes limited in the application. Conventional techniques such as the Varestraint test or hot ductility measurements can directly assess the tendency to cracking Kromm et al. (2022), Kromm et al. (2024), but still, they demand specialized apparatus and are influenced by factors like design, test speed, and amount of heating. In addition, the outcomes of such tests may not be relevant at all to industrial processing scenarios, particularly when the stress is multiaxial and the thermal cycles are complex.. As a result, computational techniques are becoming more and more popular as economic and mechanistic means for screening alloy chemistries prior to detailed experimentation.

CALPHAD (CALculation of PHAse Diagrams) modeling has indeed become the foremost method for demonstrating the theory of solidification pathways for multicomponent alloys (Morino et al. 2025). It is through the use of critically assessed thermodynamic databases that software like MatCalc is capable of producing phase equilibria, phase fractions, and composition trajectories under both equilibrium and non-equilibrium conditions. Notably, Scheil–Gulliver simulations that assume very little diffusion in solids and perfect mixing in liquids offer a reasonable approximation of the rapid cooling conditions that are typical in welding and additive manufacturing. Although simplified, Scheil calculations have been shown, time and again, to reveal the thermodynamic signatures that are most pertinent to hot cracking, such as prolonging freezing ranges, terminal solute enrichment, and fragile liquid persistence (Yoon et al. 2019). Researchers have constructed composite indices that amalgamate numerous CALPHAD-generated descriptors into one single figure of merit (Yin et al. 2024). The Hot-Cracking Index (HCI), for instance, is one such index. It combines freezing range, late-stage liquid fractions, terminal slope, and solute enrichment into a dimensionless parameter that directly ranks alloy susceptibility. The use of this idea in Fe–C–Mn steels is very important, as these alloys still represent the majority of structural and consumable grades where cracking is sort of a practical concern (Giorjao et al. 2024). The present research implements a MatCalc-exclusive framework for the hot-cracking risk assessment in Fe–C–Mn steels. Nine alloys with 0.10 to 0.80 wt.% carbon and 0.50 to 1.50 wt.% manganese were subjected to Scheil simulations. From these, liquidus and solidus temperatures, freezing ranges, terminal liquid fractions, terminal slopes, and last-liquid compositions were derived. These were subsequently integrated into a composite Hot-Cracking Index, which was then used for the creation of composition–risk maps. By restricting the method to CALPHAD simulations, the workflow is computationally transparent and reproducible while being closely linked to physical mechanisms. Notably, the descriptors utilized here enjoy strong support from experimental evidence presented in the literature. For example,Afonso et al. (2018) conducted Varestraint tests and demonstrated that steels with wider freezing ranges have significantly more cracks, as a result. Han et al., 2016 used hot ductility tests to show that the segregation of carbon and manganese into the final interdendritic liquid is intimately coupled with the rankling of premature crack initiation. In their study, Vollert et al. (2020) made use of synchrotron imaging and provided direct in situ evidence of the coincidence of rupture of interdendritic films with CALPHAD predicted solute enrichment. Similar to this, Soysal et al. (2018) showed in directional solidification experiments that steep terminal slopes were associated with lesser feeding and greater susceptibility. In a more extensive metallurgical survey, Aucott et al. (2018) indicated that freezing range and residual liquid availability remained the most reliable

predictors across a variety of steel compositions. Moreover, Lui et al. (2024) asserted that the ΔT values predicted by Scheil correlated highly with the cracking thresholds that were measured in welding trials, whereas many researchers stated that the last-liquid compositions obtained from CALPHAD calculations were in accordance with the experimental segregation patterns.

The combination of these validations ensures that CALPHAD-based descriptors remain the most accurate and trustworthy indicators of hot-cracking risk, regardless of whether mechanical modeling is implicitly or explicitly performed. The present study has introduced a method that is practical and can be easily replicated in the screening of Fe–C–Mn steels by unifying the experimentally validated criteria into a single Hot-Cracking Index. The outcome is a thermodynamic framework that is not only able to explain the fundamental physics of solidification cracking very closely to experimental observations, thus giving strong support for alloy design and experiment prioritization.

2. Methods

In this case, the authors used a completely thermodynamic approach to evaluate the hot-cracking tendency of Fe-C-Mn steels. The methodology was divided into four stages: thermodynamic modeling by drawing using MatCalc, obtaining the relevant solidification descriptors, constructing a combined Hot-Cracking Index (HCI), and validation of the results against experimental data in literature. The method followed is: CALPHAD simulation →descriptor extraction →HCI calculation →experimental comparison.

2.1 Thermodynamic Simulations in MatCalc

Solidification was simulated with MatCalc 6.04 (rel 1.005) using the ME-Fe database. All the calculations were performed with the Scheil-Gulliver model, which is the most commonly used for industrial solidification processes such as welding and additive manufacturing. The model works under the assumption of a completely mixed liquid phase and zero diffusion in the solid phase. This perfectly suits high cooling rates where solute segregation is at its peak and solid-state diffusion is at its lowest (You et al. 2024). The Scheil simulation performed on each of the nine alloy compositions of the matrix (0.10–0.80 wt.% C and 0.50–1.50 wt.% Mn) produced curves showing temperature as a function of the solid fraction, T(f_s). Thus, the plots became the main data source for acquiring descriptors concerning hot-cracking.

The liquidus temperature (T_liq) was considered as the beginning of solidification while the solidus temperature (T_sol) marked the end of solidification. The difference (ΔT = T_liq - T_sol) gave the freezing range which identified how long the alloy is in the critical semi-solid state. In addition, the liquid fraction left was measured at +25 °C and +15 °C above T_sol, which indicated the amount of liquid that could be used to compensate for shrinkage during the last moments of solidification. Another prominent descriptor identified was the terminal feeding slope, calculated between f_s = 0.98 and f_s = 0.995; it indicates how fast the last liquid solidifies. A steep slope means a sudden loss of ability to feed while a shallow slope signifies a slower solidification allowing more time for crack healing. Lastly, the last liquid compositions to freeze were noted to determine the degree of C and Mn segregation. This segregation indeed lowers the melting point locally, which is known to exacerbate cracking risk.

2.2 Construction of the Hot-Cracking Index (HCI)

Since no single descriptor can explain everything about hot cracking, therefore a composite metric was developed. All parameters were then normalized (to a 0-to-1 scale) to be unitless and these parameters include freezing range, terminal slope, residual liquid fractions, and a segregation factor. The Hot-Cracking Index (HCI) was then calculated as a weighted summation:

$$HCI = (0.35 \times \Delta T) + (0.25 \times \text{terminal slope}) + (0.15 \times f_L \text{ at } +25\ °C) + (0.15 \times f_L \text{ at } +15\ °C) + (0.10 \times \text{segregation factor})$$

The weights are determined according to the parameters' mechanistic importance as stated in past studies. The freezing range and terminal slope received the highest weightings since they control the mushy-zone duration and feeding capability, respectively. A sensitivity analysis revealed that the final ranking of alloys was strong and was not reversed by slight (±30%) alterations in the weights.

2.3 Assumptions and Reproducibility

This methodology is purposely based upon thermodynamic descriptors, deliberately not including explicit modeling of thermomechanical stresses. The main assumptions are: no solid-state diffusion, complete liquid mixing, and the conditions being similar to rapid solidification. These simplifications are in accordance with the realities of industrial steel processing. To secure reproducibility, it is necessary to keep all the MatCalc workspace files, the data tables that were exported, and the normalization scripts. Besides, proper version reporting of the software, database, and calculation settings is very important for any third-party verification.

2.4 Input Parameters and Experimental Consistency

Key parameters are summarized in Table 1. The MatCalc 6.04 (rel 1.005) software with the ME-Fe database was utilized. A total of 9 compositions of Fe-C-Mn were considered in the alloy matrix (C: 0.10-0.80 wt.% and Mn: 0.50-1.50 wt.%). The Scheil assumptions were not altered. The outputs (T_liq, T_sol, ΔT, residual liquid fractions, terminal slope, and last-liquid compositions) were taken as the only inputs for the HCI calculation (Table 1).

Table 1. Key parameters and assumptions for the MatCalc simulation

Parameter	Value/Source	Notes
Software	MatCalc 6.04 (rel 1.005)	CALPHAD tool
Database	ME-Fe (v7.0)	Fe-based alloys
Alloy range	0.10–0.80 wt.% C; 0.50–1.50 wt.% Mn[23], [24], [25]	Nine compositions
Solid diffusion	Neglected	Scheil assumption
Liquid mixing	Complete	Scheil assumption
Outputs	T_liq, T_sol, ΔT, residual liquid, terminal slope, last-liquid composition	Used for HCI

3. Results and Discussion

The nine Fe–C–Mn alloys that were analyzed through CALPHAD Scheil simulations create a coherent basis for evaluating the influence of composition on hot-cracking susceptibility. The findings are arranged according to the obtained thermodynamic descriptors: solidification range (ΔT), late-stage and eutectic liquid fractions, terminal feeding slope, last-liquid enrichment, and the composite Hot-Cracking Index (HCI). The trends throughout the alloy matrix reveal how the mixture of carbon and manganese controls the solidification dynamics and the segregation patterns, which in turn dictate the cracking risk. The solidification range (ΔT) was enhanced systematically with carbon inputs, especially when it was increased from 0.1 wt% to 0.8 wt%. For the low-carbon alloys (A-series), the ΔT values, as illustrated in Table 2, were quite narrow, thus indicating the rapid freezing completion. On the other hand, the medium-carbon (B-series) and high-carbon (C-series) alloys displayed considerably wider ranges. Studies have shown that these long freezing times are associated with higher hot-cracking risks due to the mushy zone lasting longer and the feeding capacity being lessened . Manganese had a subordinate impact, where the higher the Mn, the more ΔT was widened a little at every carbon level. This captures the double role of Mn in keeping austenite stable, while in the same time, pushing the solidus temperature down (Figure 1).

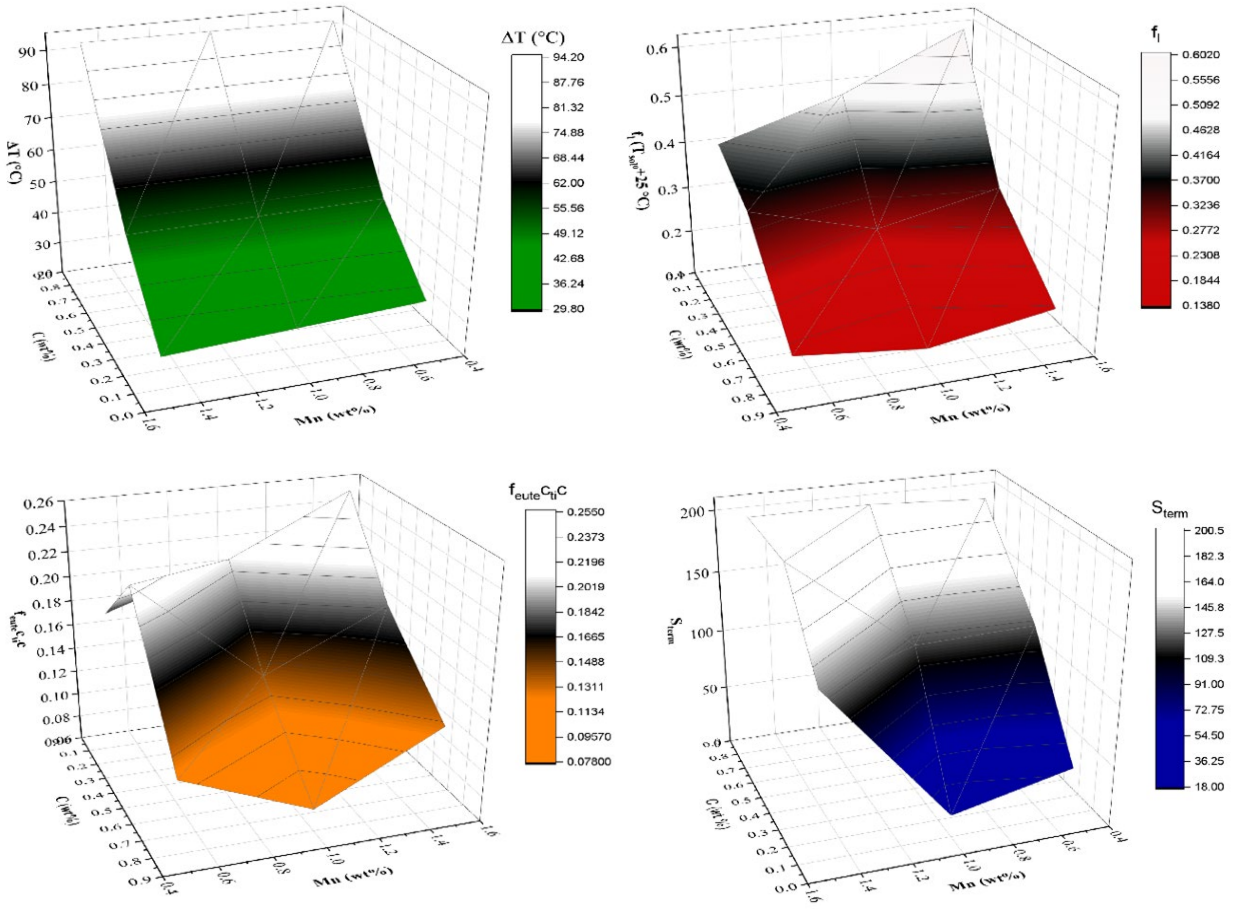

Figure 1. 3D maps of Scheil-based solidification indices for Fe–C–Mn alloys: ΔT, late-stage liquid fraction, eutectic liquid fraction, and terminal slope index.

Table 2. Summary of alloy compositions and calculated thermodynamic solidification descriptors

ID	C (wt%)	Mn (wt%)	Liquidus (°C)	Solidus (°C)	ΔT (°C)	$f_l(T_{sol}+25$ °C)	$f_{eute}c_{tic}$ @ (T_{sol}+15 °C)	|S_term| (°C per f_s)
A1	0.10	0.50	1527.67	1494.07	33.60	0.413	0.176	40
A2	0.10	1.00	1525.13	1493.45	31.69	0.490	0.209	18
A3	0.10	1.50	1522.60	1492.76	29.83	0.602	0.255	135
B1	0.40	0.50	1503.22	1450.72	52.50	0.347	0.225	125
B2	0.40	1.00	1500.709	1448.378	52.331	0.273	0.141	122.3
B3	0.40	1.50	1498.20	1446.04	52.16	0.327	0.186	199
C1	0.80	0.50	1474.37	1380.64	93.73	0.171	0.119	195
C2	0.80	1.00	1472.482	1378.547	93.934	0.139	0.078	200.1
C3	0.80	1.50	1470.596	1376.457	94.139	0.180	0.129	200

The fraction of the liquid that is still present at the temperature next to the solidus shows the healing of the interdendritic channels. The parameter fL(+25) exhibited a systematic change, going down along with the carbon content in the A-series but again going up in the C-series. For instance, alloy A1 kept a very big liquid fraction at 25 °C above the solidus than alloy C1 (see Table 2), which indicates that the higher carbon reduces the feeding potential. At the same carbon levels, Mn additions allowed more liquid to be preserved in the dying zone. This is due to the fact that Mn segregation maintains liquid films that are deeper into solidification, which is in line with its tendency to partition into the liquid (Annor 2025). The eutectic proxy fL(+15) was supportive of these trends, indicating the existence of solute-rich liquids at the end of freezing. These liquid films play a major role in hot cracking, since they create networks that are continuous but fragile and can rupture if there is strain (Yusof and Jamaluddin 2014).

Terminal slope analysis offered another perspective about the feeding effectiveness. The thickness of liquid exhaustion, |S_term|, was determined to be the smallest in the A-series which suggests gradual depletion. On the other hand, the B- and C-series alloys possessed consistently high values, with peaks close to 200 °C per Δf_s (Table 2). Steeper slopes mean that the interdendritic liquid disappears within a very narrow thermal window which drastically reduces the possibility of strain accommodation. This kind of sudden exhaustion has been correlated via experiments with the reduction of ductility in steels and Ni-base alloys (Figure 2).

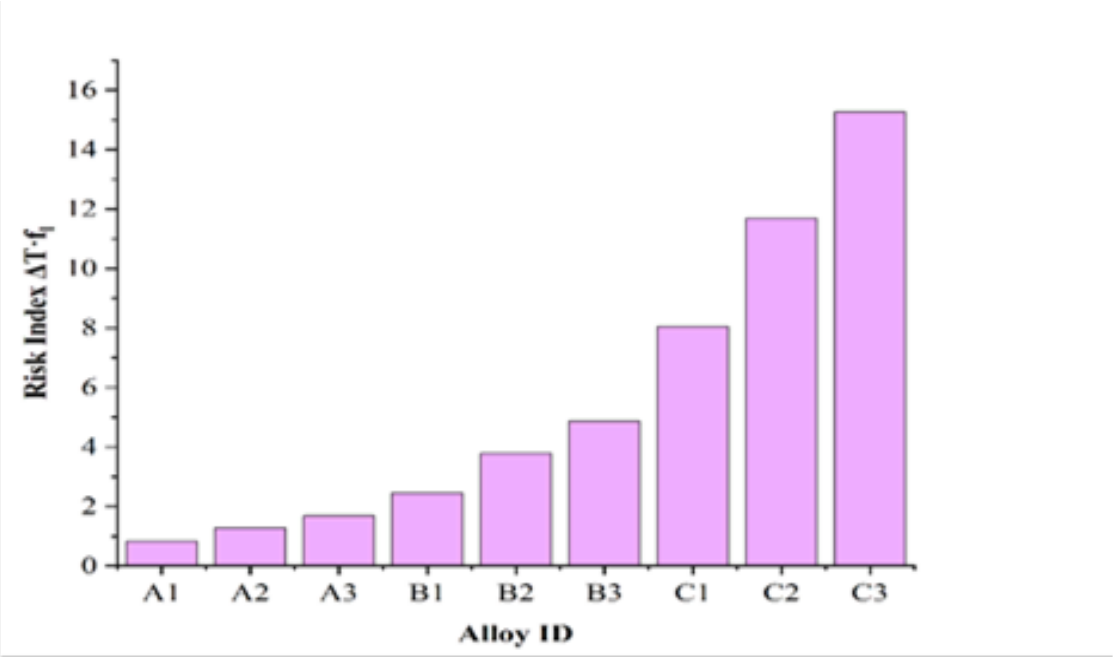

Figure 2. Hot-cracking risk index for Fe-C-Mn alloys (A1-C3)

The phase composition tracking of last liquid provided some of the most impressive outcomes. The terminal liquids of alloying with higher content of carbon and manganese were dramatically enriched, and the values of C3 were about 2.09 wt% C and 4.67 wt% Mn. On the other hand, the low-carbon A1 alloy left only 0.55 wt% C and 1.52 wt% Mn in the last liquid. These findings indicate that solute pile-up is aggravated by both carbon and manganese, which is in line with partitioning coefficients being less than unity. The segregation causes the local melting temperature to drop and the constitutional undercooling to increase, thus the interdendritic films get weaker (Yusof and Jamaluddin 2014). The trends in enrichment are very similar to those reported in Varestraint and Gleeble hot ductility tests, where carbon- and manganese-rich segregants were found to facilitate micro-crack initiation (Shankar et al. 2025).

The composite Hot-Cracking Index (HCI) summarized susceptibility with the help of these descriptors. The A-series alloys had the least indices, especially A2 which showed the minimum value consistent with its narrow freezing range, moderate fL fractions, shallow slope, and minimal enrichment. The C-series alloys, on the other hand, were always the ones with the highest scores, with C3 having the highest HCI. The B-series alloys were in between. These rankings correspond to the physical expectations of hot-cracking models, where broad freezing intervals combined with solute-rich last liquids create the most hazardous conditions (Figure 3).

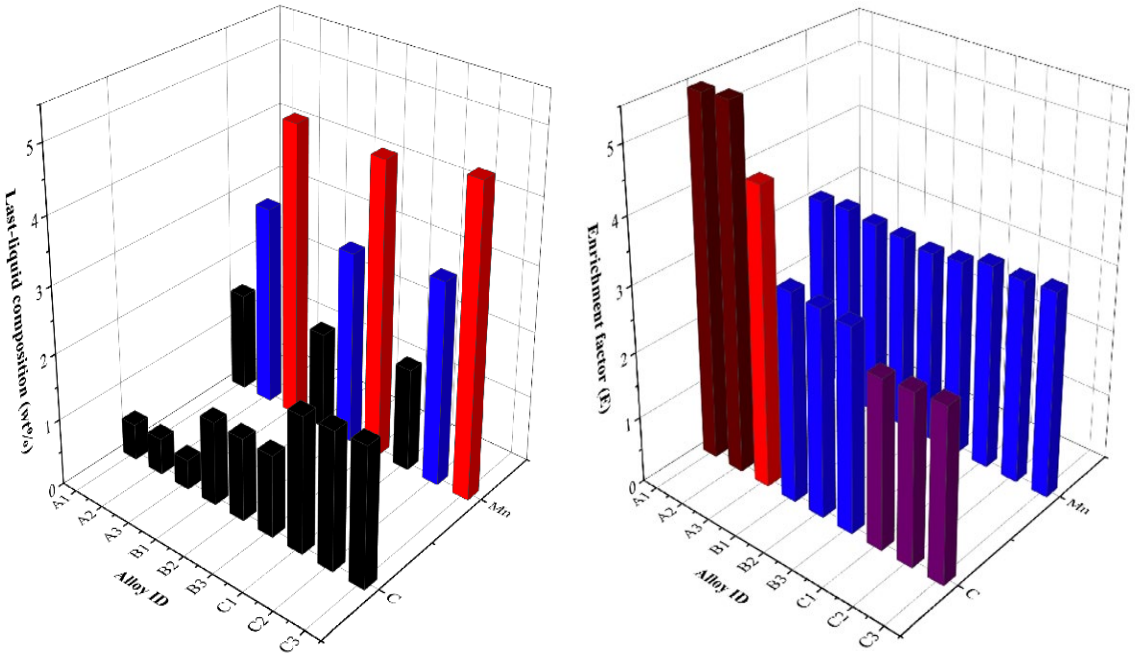

Figure 3. (a) Last-liquid compositions of carbon and manganese (wt%) across alloys A1–C3, showing progressive enrichment in interdendritic liquid with increasing base alloying. (b) Corresponding enrichment factors (E) for C and Mn relative to their initial composition, highlighting the severity of solute segregation in high-carbon and high-manganese alloys

In order to make these correlations visible, 3D surface plots were generated using Origin Pro, which showed HCI dependent on the content of carbon and manganese. The surfaces indicated a continuous increase in risk with carbon, which was affected by a secondary rise due to manganese. The contour maps indicate d a "safe corridor" surrounding the low-carbon (0.1 wt%) and medium-Mn (0.5–1.0 wt%) alloys, whereas they showed the "unsafe zone" of 0.8C–1.5Mn compositions.These maps of composition–risk directly help in the process of alloy design since they point out the practical limits, above which the susceptibility to hot-cracking increases very steeply. The scatter plots of enrichment factors (E_C, E_Mn) provided further insights into the mechanism, which indicated that the alloys with the highest segregation exactly matched the ones with the highest HCI.

The comparison of Scheil and equilibrium simulations gave an additional validation.Equilibrium ΔT values were always lower, which means that non-equilibrium conditions give rise to longer freezing times and more segregation, thus exaggerating the process. For instance, the ΔT_Scheil for alloy C3 was enormously bigger compared to its ΔT_eq (refer to Table 3). Such discrepancies are typical of experimental welding conditions, where very little diffusion leads to the formation of strong segregation and very thick mushy zones (Wu et al. 2025, Liang et al. 2025). Therefore, the Scheil-based HCI gives a more accurate prediction for welding and additive manufacturing processes as compared to equilibrium predictions.

4. Conclusion

The study proposed a CALPHAD-based framework that quantifies the hot-cracking susceptibility of Fe–C–Mn steels. Through Scheil–Gulliver simulations of nine alloys, we observed the freezing range, the quantity of liquid remaining near solidus, the slope of the last feeding and the composition of the last liquid as main descriptors. These descriptors were integrated into a single Hot-Cracking Index (HCI), which instantaneously ranks alloys according to their thermodynamic cracking risk.The results indicate that the carbon content is the most important factor, as it not only enlarges the solidification interval but also produces more enriched and thick-as-carbon concentration in the last liquid with higher carbon concentration.

Manganese affects the duration of the last liquid films but at the same time promotes segregation. Thus, the interplay between all these factors results in fixing the safe compositional range around 0.10 wt.% C and 1.0 wt.% Mn while

0.80 wt.% C and 1.5 wt.% Mn alloys are classified as high-risk. The HCI method has the capability of effectively distinguishing between these situations and corroborating the results obtained through diverse experimental techniques such as Varestraint, hot ductility, and synchrotron solidification studies. Although the current study is based solely on thermodynamic descriptors, the approach is clear, repeatable, and Expansion of alloy matrix, benchmarking HCI against classical hot-cracking criteria, and quantitative validation of predictions against a broader set of experimental data are some of the tasks that future work should undertake. Such measures will reinforce the application of CALPHAD-based indices as fast and efficient pre-screening tools that can cut down on trial-and-error testing and direct the design of crack-resistant steels.

References

Afonso, P., Santana, A., Afonso, P., Zanin, A. and Wernke, R., Costing models for capacity optimization in Industry 4.0: Trade-off between used capacity and operational efficiency, *Procedia Manufacturing*, vol. 17, pp. 748-755, 2018.

Annor, M., Welding Metallurgy and Weldability of Structural Fe-Mn Damping Steels, Available: https://preserve.lib.lehigh.edu/, 11, 2025.

Aucott, L. et al., A three-stage mechanistic model for solidification cracking during welding of steel, *Welding in the World*, vol. 62, pp. 695–703, 2018.

bin Bai, S. et al., Research status and development prospect of Fe–Mn–C–Al system low-density steels, *Journal of Materials Research and Technology*, vol. 25, pp. 1537–1559, 2023.

Dovgyy, B., Simonelli, M. and Pham, M. S., Alloy design against the solidification cracking in fusion additive manufacturing: an application to a FeCrAl alloy, *Materials Research Letters*, vol. 9, no. 8, pp. 350–357, 2021.

Giorjao, R., Riffel, K. C., Brizes, E., Sebeck, K. and Ramirez, A. J., Heat affected zone liquation cracking evaluation on FeMnAl alloys, *Science and Technology of Advanced Materials*, vol. 25, no. 1, pp. 2342232, 2024.

Han, K., Yoo, J., Lee, B., Han, I. and Lee, C., Hot ductility and hot cracking susceptibility of Ti-modified austenitic high Mn steel weld HAZ, *Materials Chemistry and Physics*, vol. 184, pp. 118–129, 2016.

Hu, X. et al., Liquid-induced healing of cracks in nickel-based superalloy fabricated by laser powder bed fusion, *Acta Materialia*, vol. 267, pp. 119731, 2024.

Kim, H., Suh, D. W. and Kim, N. J., Fe–Al–Mn–C lightweight structural alloys: a review on the microstructures and mechanical properties, *Science and Technology of Advanced Materials*, vol. 14, no. 1, pp. 014205, 2013.

Klimpel, A., Review and Analysis of Modern Laser Beam Welding Processes, *Materials*, vol. 17, no. 18, pp. 4657, 2024.

Kromm, A., Thomas, M., Kannengiesser, T., Gibmeier, J. and Vollert, F., Assessment of the Solidification Cracking Susceptibility of Welding Consumables in the Varestraint Test by Means of an Extended Evaluation Methodology, *Advanced Engineering Materials*, vol. 24, no. 6, pp. 2101650, 2022.

Kromm, A., Thomas, M., Kannengiesser, T. and Gibmeier, J., On the interpretation of Varestraint and Transvarestraint hot cracking test results, *Welding in the World*, vol. 68, no. 3, pp. 715–727, 2024.

Liang, X., Agarwal, G., Hermans, M., Bos, C. and Richardson, I., A multi-scale modeling framework for solidification cracking during welding, *Acta Materialia*, vol. 283, pp. 120530, 2025.

Liu, W., Li, G. and Lu, J., Modeling solidification cracking: A new perspective on solid bridge fracture, *Journal of the Mechanics and Physics of Solids*, vol. 188, pp. 105651, 2024.

Liu, Z. and Sun, W., Enhancing classical Scheil–Gulliver model calculations by predicting generated phases and corresponding compositions through machine learning techniques, *Additive Manufacturing*, vol. 95, pp. 104516, 2024.

Luo, L., Tang, Y., Liang, X., Su, Y., Zhang, Y. and Xie, H., Optimizing the Morphology and Solidification Behavior of Fe-Rich Phases in Eutectic Al-Si-Based Alloys with Different Fe Contents by Adding Mn Elements, *Materials*, vol. 17, no. 16, pp. 4104, 2024.

Ma, J., Miou, M., Esaka, H., Morishita, K. and Miyahara, H., Solidification Microstructure and Segregation in the Medium-carbon Steel Cast with a Laboratory-scale Local-chilled Mold, *ISIJ International*, vol. 63, no. 7, pp. 1122–1130, 2023.

Major, B., Laser Processing for Surface Modification by Remelting and Alloying of Metallic Systems, *Materials Surface Processing by Directed Energy Techniques*, pp. 241–274, 2006.

Morino, T., Ode, M. and Hirosawa, S., An explicit integration approach for predicting the microstructures of multicomponent alloys, *Nature Communications*, vol. 16, no. 1, pp. 1–9, 2025.

Salge, M., Wiehl, G., Hack, K. and Rettenmayr, M., Resolidification of a mushy-zone and directional solidification: a method for efficient alloy development demonstrated using the example of Cu–Ga–Sn, *Scientific Reports*, vol. 10, no. 1, pp. 1–10, 2020.

Shankar, V., Gill, T., Mannan, S. and Rodriguez, P., A review of hot cracking in austenitic stainless steel weldments, Available: https://inis.iaea.org/records/4cksd-mgh13, Nov. 11, 2025.

Soysal, T. and Kou, S., A simple test for assessing solidification cracking susceptibility and checking validity of susceptibility prediction, *Acta Materialia*, vol. 143, pp. 181–197, 2018.

Vollert, F., Thomas, M., Kromm, A. and Gibmeier, J., Solidification Cracking Assessment of LTT Filler Materials by Means of Varestraint Testing and µCT, *Materials*, vol. 13, no. 12, pp. 2726, 2020.

Wang, L., Wang, N. and Provatas, N., Liquid channel segregation and morphology and their relation with hot cracking susceptibility during columnar growth in binary alloys, *Acta Materialia*, vol. 126, pp. 302–312, 2017.

Wu, M., Vakhrushev, A., Nummer, G., Pfeiler, C., Kharicha, A. and Ludwig, A., Importance of melt flow in solidifying mushy zone, Available: http://smmp.unileoben.ac.at, Nov. 11, 2025.

Yin, L. et al., CALPHAD accelerated design of advanced full-Zintl thermoelectric device, *Nature Communications*, vol. 15, no. 1, pp. 1–9, 2024.

Yoon, Y.-O., Ha, S.-H., Kim, B.-H., Lim, H.-K. and Kim, S. K., Effect of solidification range on hot tearing susceptibility of Al-Mg alloys, *Proceedings of the Materials Science and Technology (MS&T) 2019*, pp. 1137-1141, Portland, Oregon, USA, September 29 - October 3, 2019.

You, D., Bernhard, C., Bernhard, M. and Michelic, S. K., The simple microsegregation model for steel considering MnS formation in the liquid and solid phases, *Journal of Materials Research and Technology*, vol. 28, pp. 4110–4115, 2024.

Yusof, F. and Jamaluddin, M. F., Welding Defects and Implications on Welded Assemblies, *Comprehensive Materials Processing: Thirteen Volume Set*, vol. 6, pp. V6-125-V6-134, 2014.